PHYSICAL REVIEW E **81**, 011607 (2010)

Asymptotic solutions for the relaxation of the contact line in the Wilhelmy-plate geometry: The contact line dissipation approach

Stanimir Iliev* and Nina Pesheva†
Institute of Mechanics, Bulgarian Academy of Sciences, Acad. G. Bonchev Street 4, 1113 Sofia, Bulgaria

Dimitar Iliev
Department of Mathematics and Informatics, Sofia University, 5 J. Bourchier Street, 1164 Sofia, Bulgaria
(Received 11 September 2009; published 26 January 2010)

The relaxation of straight contact lines is considered in the context of the Wilhelmy-plate experiment: a homogeneous solid plate is moving vertically at constant velocity in a tank of liquid in the partial wetting regime. We apply the contact line dissipation approach to describe the quasistatic relaxation of the contact line toward the stationary state (below the entrainment transition). Asymptotic solutions are derived from the differential equations describing the capillary rise height and the contact angle relaxation for small initial deviations of the height from the final stationary value in the model considering the friction dissipation at the moving contact line, in the model considering the viscous flow dissipation in the wedge, and in the combined model taking into account both channels of dissipation. We find that for all models the time relaxation of the height and the cosine of the contact angle are given by sums of exponential functions up to a second order in the expansion of the small parameter. We analyze the implications which follow when only one dissipation channel is taken into account and compare them to the case when both dissipation channels are included. The asymptotic solutions are compared with experimental results and with numerically obtained solutions which are based on hydrodynamic approach in lubrication approximation with and without a correction factor for finite contact angles. The best description of the experimental data, based on multicriteria testing, is obtained with the combined contact line dissipation model which takes into account both channels of dissipation.

DOI: 10.1103/PhysRevE.81.011607 PACS number(s): 68.03.−g, 68.08.−p, 05.90.+m

I. INTRODUCTION

The spreading of liquid on solid surface has numerous applications and that has provoked various studies employing different experimental and theoretical approaches. An important theoretical problem is the description of the dynamics of the three-phase contact line and its relation to the dynamics of the so-called inner part of the system in close vicinity of the contact line. A number of different approaches and models were suggested in the literature [1–19]. A comparison of the predictions made within the different approaches for the different geometries (drops, capillaries, Wilhelmy-plate geometry, fibers, etc.) with the available experimental data, as well as a justification of the approximations made, is among the important problems standing in front of the scientists working in this field.

For small capillary and Reynolds numbers the basic models suggested lead to a relationship between the dynamic contact angle and velocity of the contact line [19]. The studies show that it is very difficult from a comparison with the experimental results to give a preference to a specific model based on the above relation only. Taking into account this Brochard-Wyart and de Gennes [20] suggested that one should use additional criteria when comparing different models. For such additional criteria one can use, e.g., the type and the parameters of the function, describing the relaxation of the contact angle, the critical velocity at which the relaxation toward stationary state is no longer possible, etc.

There are several important questions concerning the relaxation process which need to be answered and the answers to be compared with the experiment for the different models suggested in the literature. It is important to know what kind of function describes best the relaxation process for finite values of the equilibrium contact angle for all stages of the relaxation (initial, intermediate, and final—see, e.g., [21]), what is the relaxation time, how it depends on the velocity of the plate, and what are the predictions of the linear analysis of the stability of the solutions.

In the approximation of small contact angles the asymptotic solutions in the different models and geometries lead to different power law dependencies of the dynamic contact angle on time (e.g., for a plate and fiber withdrawing from a tank of liquid in the hydrodynamic model (HDM), which focuses on the viscous flow dissipation in the wedge, it was obtained $\theta \sim t^{-1/2}$ [22,23], and in the molecular-kinetic model (MKM), which focuses on the dissipation due to the moving contact line, for a fiber it was found $\theta \sim t^{-1}$ [23]). They lead also to different critical contact angles below the entrainment transition in the case of dewetting. It is interesting to see what happens in the case of finite values of the contact angle. Thus it is important to obtain asymptotic solutions for the relaxation of the contact line beyond the assumption of small contact angles.

Here we will try to answer some of the questions raised above for one of the basic geometries studied that of a solid plate moving vertically at constant speed in a tank of liquid in the partial wetting regime by deriving and analyzing the

*stani@imbm.bas.bg
†nina@imbm.bas.bg

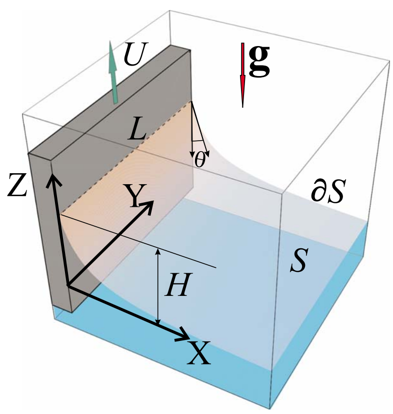

FIG. 1. (Color online) Schematic drawing of the system.

asymptotic solutions valid for arbitrary values of the contact angle. Following the work of Decker and Garoff [24] we use the term Wilhelmy-plate geometry to refer shortly to this system. Comparison between experimental data and the relations between the dynamic contact angle and the velocity for this geometry (using plate or fiber) in the different models are performed in [23,25–31]. In [31] a complex analysis and comparison are made of the predictions of a hydrodynamic approach (HA) in lubrication approximation with the experimental results for a specific system—a polydimethylsiloxane (PDMS) liquid sliding down on a fluorinated silicon surface. Recently in [32] numerical results were obtained in the framework of the contact line dissipation approach (CLDA) [12,19,33] considering only the dissipation due to the moving contact line (MKM) [2,34]. These results were compared with the experimental results in [31]. In the current work we continue our studies in the framework of the CLDA in the more general case where we take into account also the viscous flow dissipation in the wedge (HDM) [12,13,20,35].

We obtain here the asymptotic solutions for the relaxation of the contact line in the framework of the general CLDA for the Wilhelmy-plate geometry for arbitrary values of the contact angle for velocities below the entrainment transition. We consider velocities which are sufficiently small so that the motion of the meniscus can be considered quasistatic. This allows one to use the simple analytic relation which exists in equilibrium between the height of the contact line and the contact angle [36]. Complex analysis is made of the CLDA on the basis of the obtained asymptotic solutions and comparison of the predictions with the results of the HA in lubrication approximation and the complex experimental results in [31,37] is performed. We study the implications which follow when only one dissipation channel is taken into account and compare them to the case when both dissipation channels are included.

II. PROBLEM FORMULATION

We consider a partially immersed homogeneous solid plate moving vertically with constant speed U in a bath of liquid as shown in Fig. 1. The considered speeds of the plate are sufficiently small so that the motion of the meniscus can be considered quasistatic. One of the plate faces (we do not consider the other) is described with a Cartesian coordinates (Y,Z) where the Y axis is horizontal and the Z axis is directed upward as shown in Fig. 1. The liquid of density ρ forms with the air free surface S. Since the solid plate is homogenous the problem reduces to the study of the two-dimensional projection $\partial S=\{X,Z(X)\}$ of the meniscus in the (X,Z) plane. The liquid meniscus forms with the solid plate an apparent contact line L and an apparent dynamic contact angle θ. Following Voinov [3], by apparent dynamic contact angle we refer to the angle of the slope of the meniscus profile ∂S at a distance d from the vertical plate if this angle changes weakly with the contact line height relative to the liquid surface sufficiently away from the moving plate (see [19]). In quasistatic regime the same distance d can be used for which the Young equation holds for the equilibrium contact angle. The apparent contact line is defined by its rise height $H=Z(0)$ (as shown in Fig. 1). The considered velocities of the plate are suitably small so that the energy dissipation which occurs is basically in the vicinity of the contact line in the region below the scale of observation d.

In the CLDA [12] one can obtain an equation for the velocity V of the contact line relating the force responsible for the motion of the contact line and the dissipation of energy $\mathring{\Sigma}$ occurring when the contact line is moving. The motion of the contact line is due to the out-of-balance surface tension force, $F_w=\gamma(\cos\theta_{eq}-\cos\theta)$, where γ is the liquid/vapor surface tension and θ_{eq} is the apparent equilibrium contact angle. Thus using the standard mechanical description of dissipative system dynamics [21,23,38] one has

$$F_w = \partial\mathring{\Sigma}/\partial V. \tag{1}$$

When the existence of hysteresis is not taken into account θ_{eq} is given by the Young equation and whenever there is a hysteresis of the equilibrium contact angle in the interval $[\theta^r_{eq},\theta^a_{eq}]$, then for θ_{eq} in Eq. (1) one should take θ^r_{eq} or θ^a_{eq} depending on the direction of the contact line motion.

In the CLDA there are two basic approaches or models [19,21], each focusing on different channel of dissipation of energy when the contact line is moving. In the MKM the focus is on the dissipation $\mathring{\Sigma}_l$ which is due to the attachment and detachment of liquid molecules to the solid surface. At low velocities V of the contact line relaxation the expression for the dissipation function per unit length of the contact line can be written as [2,21]

$$\mathring{\Sigma}_l = \xi V^2/2, \tag{2}$$

where ξ is a friction dissipation coefficient, which has the same dimensionality as the liquid viscosity η. An expression for ξ was derived in the molecular-kinetic theory of Blake and Heynes [2]. In the HDM the emphasis is on the viscous flow dissipation $\mathring{\Sigma}_w$ which occurs basically in the vicinity of the contact line in a mesoscopic region below the scale of observation. Using Moffatt's solution [39] for the flow of a viscous fluid inside a corner, one has for $\mathring{\Sigma}_w$ per unit length of the contact line (see also Eq. 3.2 in [3])

$$\mathring{\Sigma}_w = 2\eta l V^2 \sin^2\theta/(\theta - \sin\theta\cos\theta), \tag{3}$$

where

$$l = \ln(d/d_{\min}). \tag{4}$$

η is the liquid viscosity and $d_{\min}$ is the limiting small scale down to which it is possible to approximately use the hydrodynamic description of the fluid [3]. For small contact angles $[2\eta l V^2 \sin^2\theta/(\theta-\sin\theta\cos\theta) \to 3\eta l V^2/\tan\theta]$ instead of Eq. (3) one can use the lubrication approximation [40,41] for $\mathring{\Sigma}_w$,

$$\mathring{\Sigma}_w = 3\eta l V^2/\tan\theta, \tag{5}$$

or even the simpler form, $\mathring{\Sigma}_w = 3\eta l V^2/\theta$ [12]. We denote this variant of the HDM by HDM-L (where L stands for lubrication approximation).

Taking into account Eq. (2) or (3) in Eq. (1) one has the following equations:

$$\xi V = \gamma(\cos\theta_{eq} - \cos\theta), \tag{6}$$

$$\psi_1 \sin^2\theta/(\theta - \sin\theta\cos\theta)V = \gamma(\cos\theta_{eq} - \cos\theta), \tag{7}$$

respectively, where we have set $\psi_1 = 4\eta l$. In the lubrication approximation one has instead

$$\psi_2 V \cot\theta = \gamma(\cos\theta_{eq} - \cos\theta), \tag{8}$$

where $\psi_2 = 6\eta l$.

In addition to the MKM and the HDM it is of interest to consider a model which takes into account both channels of dissipation. This is in accordance with de Gennes approach in his analysis of the dissipation in the precursor film. de Gennes suggested [12] that in the dissipation energy $\mathring{\Sigma}$ one should include all possible channels of dissipation occurring when the contact line is moving: the viscous flow dissipation $\mathring{\Sigma}_w$, the dissipation at the advancing contact line $\mathring{\Sigma}_l$, and the dissipation in the precursor film $\mathring{\Sigma}_f$. Here we do not consider the dissipation in the precursor film $\mathring{\Sigma}_f$ since it is not a generic feature in the partial wetting regime. Thus in the partial wetting regime taking into account both channels of dissipation [a combined contact line dissipation model (CLDM)] one has

$$[\xi + \psi\Phi(\theta)]V = \gamma(\cos\theta_{eq} - \cos\theta), \tag{9}$$

where

$$\Phi(\theta) = \sin^2\theta/(\theta - \sin\theta\cos\theta), \quad \psi = \psi_1, \tag{10}$$

or

$$\Phi(\theta) = 1/\cot\theta, \quad \psi = \psi_2, \tag{11}$$

in a lubrication approximation (a combined CLDM-L). Note that the parameters ξ and ψ have the same dimensionality. In the case of a plate moving with velocity U one has for the velocity V of the contact line relative to the plate,

$$V = dH/dT - U, \tag{12}$$

where T is the time. By setting $\psi=0$ or $\xi=0$ in Eq. (9) one obtains the MKM and the HDM, respectively. Equation (9) can be made dimensionless by expressing the height in terms of the capillary length l_c, $l_c = \sqrt{\gamma/\rho g}$ (g is the gravity acceleration), and the time in terms of the characteristic time,

$$\tau_0 = l_c(a\xi + b\psi)/\gamma, \quad \text{where } a \equiv \text{const}, \quad b \equiv \text{const}. \tag{13}$$

In what follows (unless specifically stated otherwise) we will work in dimensionless variables and for simplicity we will use the same symbols, but using the lower case letters, as for the dimensional variables, i.e., $h = H/l_c$, $t = T/\tau_0$, and the dimensionless plate velocity is

$$u = (a\xi + b\psi)U/\gamma. \tag{14}$$

We suppose that initially the liquid meniscus is not in a stationary state. Under the action of the surface tension and the gravity the incompressible liquid relaxes toward the stationary state dissipating energy. In the quasistationary regime the liquid meniscus $S \equiv \{x, y, z(x)\}$ is a Laplacian surface at any instant of time t. The linear sizes of the container are considered sufficiently big as compared to the capillary length l_c so that the following conditions hold for the meniscus at infinity: $z(\infty)=0$, $dz/dx|_\infty = 0$ (the container wall, opposite to the moving plate, can be considered as placed at infinity). Based on the quasistationarity assumption one can utilize the expression known from equilibrium [36] relating the instantaneous height and the dynamic contact angle of the meniscus at the moving plate

$$h = \sqrt{2(1 - \sin\theta)}, \tag{15}$$

from which we follow the expressions

$$\cos\theta = h\sqrt{4 - h^2}/2, \quad \sin\theta = 1 - h^2/2, \quad \theta = \arcsin(1 - h^2/2). \tag{16}$$

Without a loss of generality one can study the case

$$0 \le h < \sqrt{2}, \tag{17}$$

which corresponds to contact angles $0 < \theta \le 90°$ (since the following symmetry holds $h, \theta \Leftrightarrow -h, 180° - \theta$).

Taking into account the relations [Eq. (16)] expressions (10) and (11) for the function $\Phi(\theta)$ can be expressed as functions of the height h: $\Phi(\theta) \equiv \Phi[\theta(h)]$. Then from Eq. (9) the following differential equation for the height h of the contact line follows:

$$\frac{dh}{dt} = u + \frac{\gamma}{\xi + \psi\Phi(h)}\left(\cos\theta_{eq} - \frac{h}{2}\sqrt{4 - h^2}\right). \tag{18}$$

Our goal is to find asymptotic solution $h(t)$ of Eq. (18) for small initial deviations of the capillary rise height from the final stationary height h_{st} (or the equilibrium height h_{eq} in the case of a spontaneous relaxation $u=0$). After a solution is found for the contact line height $h(t)$, one can obtain the time evolution of the cosine of the contact angle using Eq. (16).

III. ASYMPTOTIC SOLUTION

A. MKM

Equation (18) takes its simplest form when $\psi=0$, $\xi \neq 0$. In this case $a=1$, $b=0$ are set and one has

$$\frac{dh}{dt} = u + (\cos\,\theta_{eq} - h\sqrt{4-h^2}/2). \tag{19}$$

We first study this simpler case. From Eq. (19), taking into account condition (17) one gets the following expression for the stationary height h_{st}:

$$h_{st} = \sqrt{2[1-\sqrt{1-(\cos\,\theta_{eq}+u)^2}]}. \tag{20}$$

When $dh/dt \neq 0$ we look for the asymptotic solution $h(t)$ of Eq. (19) in the case of small deviations $\varepsilon(t)$ from the final value h_{st} [Eq. (20)] in the following form:

$$h(t) = h_{st} + \varepsilon(t), \quad \text{where } |\varepsilon(t)| \ll 1. \tag{21}$$

From Eq. (19) an ordinary differential equation follows for $\varepsilon(t)$,

$$d\varepsilon(t)/dt = \cos\,\theta_{eq} + u - (\varepsilon + h_{st})\sqrt{1-(\varepsilon+h_{st})^2/4}. \tag{22}$$

Presenting the right-hand side of Eq. (22) as a Taylor series one has

$$d\varepsilon(t)/dt = -A\varepsilon + B\varepsilon^2 + O(\varepsilon^3), \tag{23}$$

where the constants A and B are given by

$$A = (2-h_{st}^2)/\sqrt{4-h_{st}^2}, \tag{24}$$

$$B = h_{st}(6-h_{st}^2)/[2\sqrt{4-h_{st}^2}(4-h_{st}^2)]. \tag{25}$$

Equations (24) and (25) can be expressed in the following alternative form using Eq. (16):

$$A = h_{st}\tan\,\theta_{st}, \quad B = h_{st}^2(2-\sin\,\theta_{st})/[\cos\,\theta_{st}(1-\sin\,\theta_{st})]. \tag{26}$$

We will find a solution of Eq. (23) by the perturbation technique. Considering the initial deviation $\delta=\varepsilon(0)$ to be a small parameter, we now seek a solution of Eq. (23) in the following form:

$$\varepsilon(t) = \varepsilon_1(t)\delta + \varepsilon_2(t)\delta^2 + \cdots. \tag{27}$$

In this work we will obtain only the first two terms $\varepsilon_1(t)$, $\varepsilon_2(t)$ in this expansion. It is clear that in the same way one can proceed to obtain the higher order corrections. Inserting the expansion [Eq. (27)] for $\varepsilon(t)$ into Eq. (23), we obtain to a first order in δ the equation for $\varepsilon_1(t)$,

$$d\varepsilon_1(t)/dt = -A\varepsilon_1(t), \tag{28}$$

and to a second order the equation for $\varepsilon_1(t)$ and $\varepsilon_2(t)$,

$$d\varepsilon_2(t)/dt = -A\varepsilon_2(t) + B\varepsilon_1^2(t). \tag{29}$$

The appropriate boundary conditions are

$$\varepsilon_1(0) = 1, \quad \varepsilon_2(0) = 0. \tag{30}$$

The integration of Eqs. (28)–(30) gives

$$\varepsilon_1(t) = \exp(-At), \tag{31}$$

$$\varepsilon_2(t) = -\exp(-At)[\exp(-At)-1]B/A. \tag{32}$$

By substituting back in Eq. (27) $\varepsilon_1(t)$ and $\varepsilon_2(t)$ we obtain for $h(t)$ (up to a second order of the small parameter δ) the final expression,

$$h(t) = h_{st} + \exp(-At)\delta - \exp(-At)[\exp(-At)-1]B/A\,\delta^2 + O(\delta^3). \tag{33}$$

After inserting $h(t)$ in Eq. (16) an exponential time dependence follows also for the cosine of the contact angle, $\cos\,\theta$, with the same relaxation times

$$\cos\,\theta = \cos\,\theta_{eq} + u + A\exp(-At)\delta + B\exp(-At)[2\exp(-At)-1]\delta^2 + O(\delta^3). \tag{34}$$

B. General case

It appears that in the general case of a combined CLDM starting from Eq. (18), one can proceed in exactly the same way as in the case $\xi \neq 0$, $\psi=0$ to obtain the stationary solution h_{st} and the asymptotic solution $h(t)$ in the neighborhood of h_{st}, respectively. The expression of the stationary height h_{st} in terms of the parameters (U,θ_{eq},ξ,ψ) is very long and cumbersome and is difficult to analyze. [For example in the combined CLDM-L h_{st} is a solution of an algebraic equation of fourth order in h_{st}^2, depending on the parameters $(U,\theta_{eq},\xi,\psi_2)$.] That is why we use here another approach for practical applications (see Sec. IV) which allows a compact expression of the asymptotic solution. We achieve this by changing the order $(U,\theta_{eq},\xi,\psi) \Rightarrow h_{st} \Rightarrow \varepsilon(t)$ used in the case $\psi=0$ in which h_{st} and $\varepsilon(t)$ are calculated consecutively for given values of the parameters (U,θ_{eq},ξ,ψ). Instead of this, for given values of the parameters (θ_{eq},ξ,ψ) and for every value of h_{st} in the interval $0 < h_{st} < \sqrt{2}$ one gets the dimensionless velocity u and then finds the dimensional velocity U, i.e., one has $h_{st} \Rightarrow u \Rightarrow U$; then one obtains the asymptotic solution $\varepsilon(t)$: $h_{st} \Rightarrow \varepsilon(t)$, i.e., $h_{st} \Rightarrow u(h_{st}) \Rightarrow \varepsilon(t,h_{st})$. That is instead of the explicit dependence $h(t,U)$ of the asymptotic solution on U, here we obtain an implicit relation between the asymptotic solution and the dimensional velocity of the plate $h(t,h_{st})$, $U=U(h_{st})$. In this case for expressing the variables and Eq. (18) in dimensionless form we use the following settings in Eq. (13):

$$a = 1, \quad b = \Phi(\theta_{st}) = \Phi(h_{st}).$$

The dimensionless equation [Eq. (18)] is then written as

$$\frac{dh}{dt} = u + \left(\frac{\xi}{\psi} + \Phi(h_{st})\right)\left(\cos\,\theta_{eq} - \frac{h}{2}\sqrt{4-h^2}\right)\Big/\left(\frac{\xi}{\psi} + \Phi(h)\right) \tag{35}$$

and its stationary solution h_{st} can again formally be given by expression (20). Note that the parameter ξ/ψ is a dimensionless quantity. From here for the dimensionless velocity in the stationary state one has

$$u = \frac{1}{2}h_{st}\sqrt{4 - h_{st}^2} - \cos\theta_{eq}. \tag{36}$$

The dimensional velocity U ($h_{st} \Rightarrow u \Rightarrow U$) is obtained using Eq. (14) which now takes the following form:

$$U = \left(\frac{1}{2}h_{st}\sqrt{4 - h_{st}^2} - \cos\theta_{eq}\right)\gamma/[\xi + \psi\Phi(h_{st})]. \tag{37}$$

The asymptotic solution $h(t)$ of Eq. (33) is also presented by Eqs. (21) and (22) and the final solution is given by Eq. (33), where the coefficients A and B are now different and given by the following expressions [using Eq. (16)]:

$$A = h_{st}\left\{\tan\theta_{st} + 2(\cos\theta_{eq} - \cos\theta_{st})\frac{\Phi(\theta_{st})\sin\theta_{st}[\tan\theta_{st}\Phi(\theta_{st}) - 1]}{\xi/\psi_1 + \Phi(\theta_{st})}\right\}, \tag{38}$$

$$B = \frac{4(1-\sin\theta_{st})\Phi(\theta_{st})[\tan\theta_{st}\Phi(\theta_{st}) - 1]}{\cos\theta_{st}[\xi/\psi_1 + \Phi(\theta_{st})]} + \frac{(1-\sin\theta_{st})^2(2+\sin\theta_{st})}{2\cos^3\theta_{st}} + \frac{(\cos\theta_{eq} - \cos\theta_{st})\Phi(\theta_{st})}{\xi/\psi_1 + \Phi(\theta_{st})} \times\left\{\frac{8(1-\sin\theta_{st})\Phi(\theta_{st})}{\sin^2\theta_{st}}\left[\frac{(\tan\theta_{st}\Phi(\theta_{st}) - 1)^2}{\xi/\psi_1 + \Phi(\theta_{st})} + \tan\theta_{st}\right] - \frac{(2-3\sin\theta_{st})}{\sin^2\theta_{st}} - \frac{8\Phi^2(\theta_{st})}{(1+\sin\theta_{st})} + \frac{(4 - \sin\theta_{st} - 3\sin^2\theta_{st})\Phi(\theta_{st})}{(1+\sin\theta_{st})\cos\theta_{st}\sin\theta_{st}}\right\}. \tag{39}$$

In the lubrication approximation one has

$$A = h_{st}\{\tan\theta_{st} - (\cos\theta_{eq} - \cos\theta_{st})/[(\xi/\psi_2 + \cot\theta_{st})\sin^2\theta_{st}\cos\theta_{st}]\}, \tag{40}$$

$$B = \frac{h_{st}^4(6 - h_{st}^2)}{16\cos^3\theta_{st}} + \frac{h_{st}(\cos\theta_{eq} - \cos\theta_{st})(5h_{st}^2 - 18)}{2(\xi/\psi_2 + \cot\theta_{st})(4 - h_{st}^2)^{3/2}\sin^3\theta_{st}} + \frac{4\sin\theta_{st}^3 - h_{st}^2(4 - h_{st}^2)\cos\theta_{st} + 4\cos\theta_{eq}}{(\xi/\psi_2 + \cot\theta_{st})^2\sin^4\theta_{st}(4 - h_{st}^2)}, \tag{41}$$

respectively. Equations (33) and (34) will then represent the asymptotic solutions for the relaxation of the height and the cosine of the contact angle in this case.

If now in Eqs. (38) and (39) one simply sets $\xi=0$ the corresponding expressions for the coefficients A and B will be obtained for the HDM. From Eqs. (40) and (41) by setting $\xi=0$ one gets the coefficients A and B for the HDM-L, respectively.

IV. ANALYSIS AND DISCUSSION

A. Limits of applicability of the solutions

The asymptotic solutions found for the height relaxation of the contact line [Eq. (33)] and the cosine of the contact angle [Eq. (34)] are sums of exponential functions. For initial perturbations of the order of ~10–20 % from the stationary height h_{st} the first two terms in the expansion of the asymptotic solution give very good approximation of the solution of the differential equations describing the relaxation of the height and the contact angle for all models considered (the MKM, the HDM, and the combined CLDM). This shows that the range of applicability of the asymptotic solutions is sufficiently big so that a comparison with the experimental data is possible as for the final stages of the relaxation as well as for the intermediate times for which linear, power, and single exponent functions have been suggested (for details see [21]).

In the case of a spontaneous relaxation ($u=0$), for small dynamic contact angles and zero equilibrium contact angle, using the approximate expressions,

$$\partial h/\partial\theta \approx -1/2, \quad \cos\theta \approx 1 - \theta^2/2, \quad \tan\theta \approx \theta, \tag{42}$$

from Eq. (18) one gets

$$\frac{d\theta}{dt} \approx -\frac{1}{4}\gamma\theta^2/(\xi + \psi/\theta). \tag{43}$$

From here one approximately also obtains power dependencies of the dynamic contact angle on time $\theta \approx t^{-1}$ and $\theta \approx t^{-1/2}$ for the MKM and for the HDM, respectively [22,23]. As one can see the approximations [Eq. (42)] are no good at finite contact angles therefore for finite contact angles the power dependence on time is not a good approximation of the solution of Eq. (18). The difference in the powers of the power dependencies in time in approximation of small contact angles of the solution of Eq. (18) for the MKM and the HDM is used for experimental identification of the dominant dissipation channel influencing the dynamics of the contact angle. A difference between the MKM and the HDM is also observed in the obtained asymptotic solutions. Going back to dimensional quantities one gets that the relaxation rates (the inverse of the relaxation time $\sigma=1/\tau$) for the MKM and for the HDM are proportional to θ and θ^2, respectively. (Note that the coefficient A [Eq. (23)] is actually the dimensionless relaxation rate $\sigma=A$.) In the obtained asymptotic solution the relaxation rates for the MKM and the HDM differ also for finite contact angles. This difference manifests itself very clearly in the analysis of the variation of the relaxation rate σ with the velocity of the plate. We will return to this problem also in Sec. IV C where we apply our results to a specific experimental system [31].

B. Linear stability analysis

Linear stability analysis for the combined CLDM-L was performed by Golestanian and Raphaël [42] for $\theta_{eq} \ll 1$. Here, we perform linear stability analysis for finite equilibrium contact angles by the help of the obtained expressions for A (or σ). The obtained expressions for the asymptotic solutions for $h(t)$ and $\cos\,\theta(t)$ describe a relaxation toward a stable stationary state only for $A>0$. From here we can determine the maximal value of the velocity u of the plate for which a relaxation toward stationary state exists and from which accordingly we can determine the maximal attainable stationary height of the meniscus. In order to point out the qualitative differences between the different models we consider consecutively the MKM, the HDM, and the combined CLDM.

1. MKM

In the case when $\psi=0$ (the MKM), as follows from Eq. (26) the coefficient A can be written as

$$\sigma \equiv A = \frac{h_{st}}{\cot\,\theta_{st}}. \tag{44}$$

As one can see, A is always positive since $0 \le h < \sqrt{2}$ [Eq. (17)] and $\cot\,\theta > 0$ [Eq. (16)]. A reaches zero at height $h^*_{st} = \sqrt{2}$ at zero stationary contact angle. Therefore as follows from Eqs. (15) and (20), the dimensionless critical velocity u^*, at which a relaxation toward a stationary state is no longer possible when the plate is being withdrawn from the tank of liquid, is

$$u^* = 1 - \cos\,\theta_{eq}. \tag{45}$$

These are the critical quantities for the MKM. The stationary states corresponding to contact line heights less than $\sqrt{2}$ and nonzero stationary contact angles are stable with respect to symmetrical perturbations of the contact line, i.e., perturbations for which the contact line remains parallel to that of the stationary state (for the given velocity of the plate) but its height is above or below the stationary height. In contrast the experimental studies in [31,43] show that stationary solutions cease to exist before the contact angle reaches zero value.

2. HDM

When $\psi \ne 0$, $\xi=0$ the coefficient A in the lubrication approximation [see Eq. (40)] can be written in the following form:

$$A = \frac{h_{st}}{\sin\,\theta_{st}\cos^2\,\theta_{st}}(\cos\,\theta_{st}\sin^2\,\theta_{st} - u). \tag{46}$$

The sign of A is determined by the sign of the term in the braces,

$$A_0 = \cos\,\theta_{st}\sin^2\,\theta_{st} - u. \tag{47}$$

If $u>0$ the sign of A_0 [Eq. (47)] is always negative for $\theta_{st}=0°$ [see Eqs. (1) and (17)]. Thus it follows that with increasing the velocity of the plate u the solution looses stability before the stationary angle becomes 0° and before the stationary height could reach the value $\sqrt{2}$, respectively. In the approximation of small contact angles Eq. (47) is approximately written as

$$A_0 \approx \theta^2_{st} - \frac{\theta^2_{eq} - \theta^2_{st}}{2}. \tag{48}$$

From there it follows that A_0 and therefore A become zero at critical stationary contact angle,

$$\theta^*_{st} = \theta_{eq}/\sqrt{3}. \tag{49}$$

This is in agreement with the result of de Gennes [35] and also with the result of Golestanian and Raphaël [42].

Without the assumption of small contact angles from Eq. (39) one can obtain a relation between θ^*_{st} and θ_{eq} in the following form:

$$\theta_{eq} = \arccos(0.5/\{[1 - \tan\,\theta^*_{st}\Phi(\theta^*_{st})]\cos\,\theta^*_{st}\} + \cos\,\theta^*_{st}), \tag{50}$$

and for HDM-L from Eq. (40) one has

$$\theta^*_{st} = \arccos\sqrt[3]{\cos\,\theta_{eq}}. \tag{51}$$

The value of the critical stationary velocity can be determined from Eq. (18) by setting the left-hand side to zero, i.e.,

$$0 = u^* + \frac{\gamma}{\xi + \psi\Phi(\theta^*_{st})}(\cos\,\theta_{eq} - \cos\,\theta^*_{st}).$$

By inserting $\cos\,\theta^*_{st}$ from Eq. (50) or (51) in it then the value of the critical velocity follows for the HDM and the HDM-L, respectively, expressed in terms of the equilibrium contact angle. In the same way one can proceed to find u^* for the combined CLDM from Eq. (53) and (54) (see below).

The two dependencies $\theta^*_{st}(\theta_{eq})$, given by Eqs. (50) and (51), are shown in Fig. 2 with short dot and solid lines, respectively. The linear dependence [Eq. (49)] obtained by de Gennes is shown with a dashed line. One can see that for small contact angles all three lines are very close. For bigger contact angles the HDM leads to dependence $\theta^*_{st}(\theta_{eq})$ very close to the linear while in the lubrication approximation there is a strong nonlinear increase (see Fig. 2).

3. Combined CLDM

A relation between the critical stationary contact angle θ^*_{st} and θ_{eq} for the combined model can be obtained as in the previous case. For small contact angles result [Eq. (49)] holds true. In this case for A_0 instead of Eq. (48) one has

$$A_0 = \frac{\xi}{\psi_2}\theta^3_{st} + \theta^2_{st} - \frac{\theta^2_{eq} - \theta^2_{st}}{2} + O(\theta^4_{st}). \tag{52}$$

After elimination of the terms of third order one again obtains the relation [Eq. (49)] for the critical stationary contact angle.

Without the assumption of small contact angles from Eq. (38) one obtains

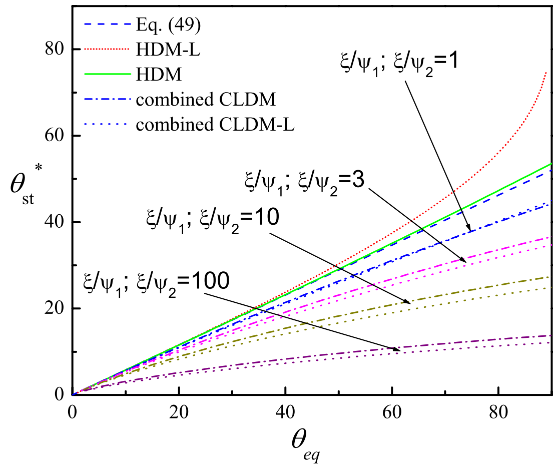

FIG. 2. (Color online) Critical value of the stationary contact angle θ_{st}^{*} as a function of the equilibrium contact angle θ_{eq} (both given in degrees). For the HDM the solid line; for the HDM-L short dotted line. For the combined CLDM and the combined CLDM-L the dashed-dotted and the dotted lines, respectively, for several values of the parameters ξ/ψ_1, ξ/ψ_2. The de Gennes result [Eq. (49)] is shown with the dashed line.

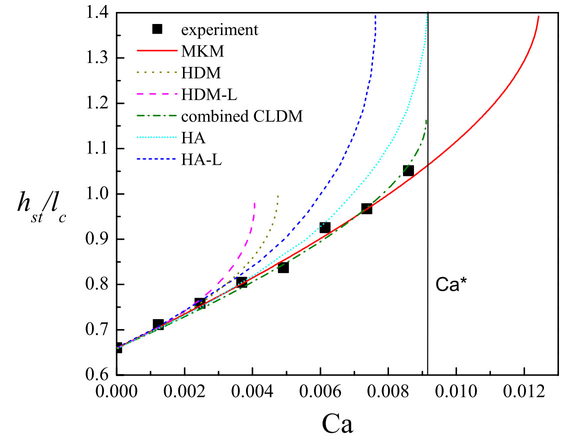

FIG. 3. (Color online) Dimensionless height of the contact line as a function of the plate velocity (expressed in terms of the dimensionless capillary number $Ca=u\eta/\gamma$): experimental results—solid squares, squares with error bars; the MKM—solid line; the HDM—dotted line; the HDM-L—dashed line; the combined CLDM ($\xi/\psi_1=9.091$) and the combined CLDM-L ($\xi/\psi_2=6.66$)—dashed-dotted lines; HA—short dotted line; and HA-L—short dashed line.

$$\theta_{eq} = \arccos([\xi/\psi_1 + \Phi(\theta_{st}^{*})]/\{2\Phi(\theta_{st}^{*}) \times\cos\theta_{st}^{*}[1-\tan\theta_{st}^{*}\Phi(\theta_{st}^{*})]\} + \cos\theta_{st}^{*}), \quad (53)$$

and for the combined CLDM-L from Eq. (40) one has

$$\theta_{eq} = \arccos(\cos\theta_{st} - \xi/\psi_2\sin^3\theta_{st} - \cos\theta_{st}\sin^2\theta_{st}). \quad (54)$$

In the combined model the relation $\theta_{st}^{*}(\theta_{eq})$ depends on the ratio ξ/ψ. For values of $\xi/\psi \ll 1$ the dependencies are very close to the dependencies in the HDM and HDM-L, respectively. The dependencies which follow from Eqs. (53) and (54) of θ_{st}^{*} on θ_{eq} are shown in Fig. 2 with dashed-dotted and dotted lines, respectively, for $\xi/\psi_1;\xi/\psi_2=1,3,10,100$. There are two special features in the behavior of $\theta_{st}^{*}(\theta_{eq})$ which one can observe in Fig. 2. First, at fixed value of the equilibrium contact angle θ_{eq}, the critical value θ_{st}^{*} decreases with increasing the ratio ξ/ψ. The maximal value of θ_{st}^{*} in the interval $[0,90°]$ decreases with increasing the ratio ξ/ψ and at $\xi/\psi=100$ it is $\sim 12°$, at $\xi/\psi=10\,000$ it is $\sim 2.5°$. For finite values of the contact angle θ_{eq} in the combined CLDM (without a complete domination of the one of the parameters ψ or ξ) one obtains a finite critical contact angle $\theta_{st}^{*}>0$. The asymptotic approach toward a zero critical contact angle with increasing ξ/ψ is quite slow. Second, the dependencies $\theta_{st}^{*}(\theta_{eq})$ in the combined CLDM and in the combined CLDM-L are very close to each other for a fixed value of the parameter ξ/ψ. One can obtain the one dependence from the other by simply changing slightly the value of ξ/ψ. For example, the dependence $\theta_{st}^{*}(\theta_{eq})$ in the combined CLDM-L at $\xi/\psi_2=10$ coincides with the dependence $\theta_{st}^{*}(\theta_{eq})$ in the combined CLDM at $\xi/\psi_1=13.5$.

For a nonzero critical stationary contact angle the critical stationary height is strictly less than $\sqrt{2}$ [see Eq. (16)]. In other words in the case when one considers the MKM one obtains that the contact angle goes continuously to zero at the maximal height $\sqrt{2}$ with increasing the plate velocity (second-order phase transition as noted by Golestanian and Raphaël [42]), while in the case when one considers the HDM or HDM-L one gets that the contact angle changes with a jump. We find here that the latter holds true also for the combined CLDM.

C. Comparison with experimental data

The obtained asymptotic solutions for the relaxation of the contact line (the height, the cosine of the contact angle, and the relaxation rate as functions of the plate velocity) as well as the obtained solutions for the critical plate velocities allow one to perform a multicriteria testing of the different models—the MKM, the HDM, and the combined CLDM. For comparison with experimental data we use the data in [31] where one can find information for all above mentioned functions.

In Ref. [31] experimental results are presented for the case when a solid plate is withdrawn with velocity U from a bath of liquid. The plate is cut from a silicon wafer (siltronix) covered with a thin layer of fluorinated material. The liquid used in the experiment in Ref. [31] is PDMS with dynamic viscosity $\eta=4.95$ Pa s, surface tension $\gamma=20.3$ mN/m, and density $\rho=970$ kg/m^3. The capillary length of the PDMS is $l_c=1.46$ mm. The PDMS wets partially the fluorinated coating with a static receding angle $\theta_{eq}^{r}=51.5°$. The dependence of the dimensionless stationary height h_{st} as a function of the dimensionless velocity given by the capillary number $Ca=U\eta/\gamma$ is shown in Fig. 2 in Ref. [31]. These results are shown for the sake of convenience also here in Fig. 3 with solid squares. The experimental studies show that the relaxation of the height of the contact line is well described by exponential decay function for velocities below the critical.

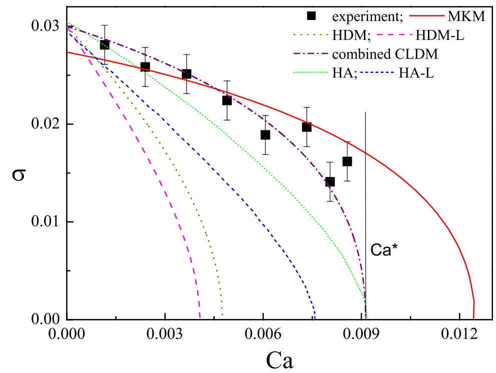

FIG. 4. (Color online) Dimensionless relaxation rate σ as a function of the capillary number Ca: experimental results—solid squares with error bars; the MKM results—solid line; the HDM results—dotted line; the HDM-L results—dashed line; combined CLDM ($\xi/\psi_1=9.091$) and the combined CLDM-L ($\xi/\psi_2=6.66$)—dashed-dotted lines; HA—short dotted line, and HA-L—short dashed line within the experimental error interval. This criterion determines uniquely $h_{st}(\mathrm{Ca})$ and $\sigma(\mathrm{Ca})$ in the MKM and in the HDM. By extrapolating the experimental results in [31] for $\sigma(\mathrm{Ca})$ to zero plate velocity we require that it lies in the interval $[0.029-0.0025, 0.029+0.0025]$.

The experimentally obtained dependence in Ref. [31] of the relaxation rate on the plate velocity below the entrainment transition is reproduced here in Fig. 4 with solid squares with error bars indicating the variation in the experimental results. In this figure the dimensionless relaxation rate is $\sigma=\eta l_c/(\tau\gamma)$ and the dimensionless velocity is given by the capillary number Ca. In [31] also the critical velocity is determined $\mathrm{Ca}^*=9.1\times10^{-3}$, at critical height $h_{st}^*\approx1.1$, and nonzero critical contact angle $\theta_{st}^*\sim23°$.

We will compare these data with the predictions of the different models (the MKM, the HDM, and the combined CLDM). The use of the experimental value of $\theta_{eq}^r=51.5°$ in the CLDA leads to that the results of all above models coincide with the experimentally determined value of h_{eq}. In the MKM and in the HDM one has one adjustable parameter: ξ or ψ, respectively; in the combined CLDM one has two adjustable parameters: ξ and ψ (there is no overdetermination of the parameters [19]). We present here results for which we have used the requirement that the solutions should have relaxation rate at zero plate velocity $\sigma(0)$ within the experimental error interval. This criterion determines uniquely $h_{st}(\mathrm{Ca})$ and $\sigma(\mathrm{Ca})$ in the MKM and in the HDM. By extrapolating the experimental results in [31] for $\sigma(\mathrm{Ca})$ to zero plate velocity we require that $\sigma(0)$ lies in the interval $[0.029-0.0025, 0.029+0.0025]$. For the determination of the additional parameter (in the combined CLDM) one should use additional criterion, e.g., how close are the dependencies $h_{st}(\mathrm{Ca})$, $\sigma(\mathrm{Ca})$ to the experimentally determined, that $\sigma(\mathrm{Ca}^*)=0$, etc. Here we impose the requirement that $\sigma(\mathrm{Ca}^*)=0$ for the determination of the second parameter in the CLDM. Of course, one can use different additional criteria.

In Figs. 3 and 4 we show the obtained dependencies for the stationary height of the contact line, $h_{st}(\mathrm{Ca})$, and the relaxation rate, $\sigma(\mathrm{Ca})$, respectively, as functions of the plate velocity (given in terms of the dimensionless capillary number Ca) for the different models.

The best fit for the MKM leads to $\sigma(0)=0.029-0.0025$ (the lower end of the interval). As one can see from Figs. 3 and 4—solid lines, the MKM reproduces well the experimental data on $h_{st}(\mathrm{Ca})$ and $\sigma(\mathrm{Ca})$ but leads to a value of the critical velocity which is 40% higher than the experimentally obtained value. In this model, as was shown in Sec. IV B 1, the stationary state is stable for dimensionless height up to $\sqrt{2}$ and zero contact angle which contradicts the experimental results.

The HDM best fit gives $\sigma(0)=0.029+0.0025$ (upper end of the interval). It does not reproduce well the experimental results on $h_{st}(\mathrm{Ca})$ and $\sigma(\mathrm{Ca})$. It leads to a value of the critical speed which is two times smaller than the one found experimentally. The HDM-L (shown with dashed line) leads to even worse description of the experimental results than the HDM (dotted line). Even if one determines the adjustable parameters of the HDM by fitting only the data on $h_{st}(\mathrm{Ca})$ [without trying to get a good reproduction of the results on $\sigma(\mathrm{Ca})$ at the same time] one still gets a poorer description of the $h_{st}(\mathrm{Ca})$ dependence than the one obtained by the MKM.

In the MKM and in the combined CLDM for the PDMS sliding on a fluorinated siltronix surface the friction coefficient ξ is about 25–35 times bigger than the viscosity η. The additional adjustable parameter ξ/ψ in the combined CLDM is determined from the requirement that $\sigma(\mathrm{Ca}^*)=0$ at the experimentally determined critical velocity $\mathrm{Ca}^*=9.1\times10^{-3}$.

For the combined CLDM this leads to $\xi/\psi_1=9.091$ and for the combined CLDM-L one gets $\xi/\psi_2=6.66$. The obtained dependencies of $h_{st}(\mathrm{Ca})$ and $\sigma(\mathrm{Ca})$ in the combined CLDM and the combined CLDM-L are shown in Figs. 3 and 4, respectively, with dashed-dotted lines. They are practically indistinguishable. Therefore for the combined model one can use the lubrication approximation for finite contact angles for large values of ξ/ψ. As one can see the agreement of the results of the combined CLDM with experimental results is significantly improved as compared to the pure MKM and HDM models for all the three criteria [i.e., $h_{st}(\mathrm{Ca})$, $\sigma(\mathrm{Ca})$, and $\mathrm{Ca}^*=9.1\times10^{-3}$]. The determination of the adjustable parameters of the combined models through the experimental values of θ_{eq}, $\sigma(0)$, and Ca^* is unique and allows one to determine the relative influence of the two dissipative channels when the contact line is moving. Thus for the ratio $\mathring{\Sigma}_l/\mathring{\Sigma}_w$ (the MKM versus the HDM channel of dissipation) one gets the following relation:

$$\mathring{\Sigma}_l/\mathring{\Sigma}_w=\xi/[\psi_1\sin^2\theta/(\theta-\sin\theta\cos\theta)].$$

For a spontaneous relaxation one obtains $\mathring{\Sigma}_l\approx6\mathring{\Sigma}_w$ and with increasing the plate velocity this ratio decreases reaching the ratio $\mathring{\Sigma}_l\approx2.5\mathring{\Sigma}_w$ at the critical velocity.

The predictions of the hydrodynamic approach (which is actually in lubrication approximation with a correction factor for finite contact angles [44]) and of the HA in lubrication approximation (denoted by HA-L) are studied also in [31,37]. The adjustable parameters in these models (the slip length l_s and the microscopic contact angle θ_m) are determined by using also the data on $[\theta_{eq}^r,\theta_{eq}^a]$ and $\sigma(0)$ at zero plate velocity. The obtained dependencies for the height h_{st}(Ca) and the relaxation rate σ(Ca) on the capillary number are shown in Figs. 4a and 8a in [37] for the HA-L and in Figs. 2a and 8b in [31] for the HA. For a more convenient comparison we reproduce these dependencies also here (only for the case $\theta_m=\theta_{eq}^r=51.5°$) in Figs. 3 and 4 with short dotted (HA) and short dashed (HA-L) lines. One can see that the HA-L leads to a worse description of the experimental results than the HDM. The results of the HA do not agree so well with the experimental results for the relaxation rate σ(Ca) at higher plate velocities as compared to the results of the combined CLDM used in the present work. Critical assumption in [31,37] is that the microscopic contact angle θ_m does not depend on the value of the capillary number. Several curves for h(Ca) and σ(Ca) are shown in [31] corresponding to different values of the microscopic contact angle. In [3,26] a combined model is studied and it is assumed that the microscopic contact angle varies with Ca. This realization again does not lead to a good description of the experimental results as noted in [45]. One may conclude that the combined model, based on the HA, does not lead to a good description of the experimental results in contrast to the good agreement found for the results of the combined CLDA used in the present work.

V. CONCLUSION

In this work we derive the asymptotic solutions for the quasistatic relaxation of the contact line in the Wilhelmy-plate geometry in the framework of the CLDA. We consider the general case of a forced relaxation when the contact line relaxes toward a stationary state when a solid plate is moving vertically at constant speed below the entrainment transition. The asymptotic solutions found here are valid for arbitrary equilibrium contact angles while the existing so far asymptotic solutions for all approaches were derived for small contact angles. Also they give very good approximation of the solutions of the differential equations describing the relaxation of the height of the contact line and of cosine of the contact angle for large deviations (of the order of 10–20 %) from the stationary state. In the framework of the CLDA we obtain asymptotic solutions in the case where the viscous dissipation term is determined from Moffatt's solution [39] for the flow of a viscous fluid inside a corner.

We consider the MKM, the HDM, and the combined CLDM in which both dissipation channels are taken into account. The obtained asymptotic solutions clearly show the qualitative difference between the MKM and the HDM. The asymptotic solutions found here for the relaxation of the height of the contact line and for the cosine of the contact angle are sums of exponential functions in all above models. These asymptotic solutions are very similar to the asymptotic solutions found previously in the framework of the CLDA for the quasistatic relaxation of the radius and the cosine of the contact angle of sessile drop in Ref. [41]. Our analysis shows that it is essential that the experimental data are fitted by a sum of exponential functions when studying the applicability of the CLDA.

We point out the implications which follow from the asymptotic solutions when only one dissipation channel is taken into account and compare them to the case when both dissipation channels are included. It is shown here that for all values of the equilibrium contact angle in the MKM the critical height reaches $h_{st}^*=\sqrt{2}$ and the contact angle goes continuously to zero (as in a second-order phase transition) with the plate speed. In the case of a HDM the relation $\theta_{st}^*=\theta_{eq}/\sqrt{3}$ is valid only for small contact angles, for finite contact angles there is a significant departures from this relation, and the critical height is strictly less than $\sqrt{2}$. The entrainment transition in the HDM can be considered as a dynamic first-order phase transition (with respect to the change of the dynamic contact angle with the plate speed). The same holds true also for the combined CLDM.

In this work we continue the studies in Refs. [20,31,37,42] aimed toward a more precise investigation of the dynamic contact angle where in addition to its dependence on the plate velocity also the relaxation time, the dependence of the relaxation time on the plate velocity, and the critical velocity are taken into account for performing of a multicriteria testing. We have applied the obtained asymptotic solution to the specific system studied experimentally in Ref. [31]. The asymptotic solution agrees with the exponential relaxation of the height found there. Fits of the experimental data on the relaxation rate as a function of the velocity are made in the MKM, in the HDM, and in the combined CLDM. Comparison of these fits shows, as should be expected [19], that a best description of all the experimental data is obtained with the combined CLDM. The HDM does not reproduce well the experimental data on σ(Ca) since the relaxation rate decreases too fast with the plate speed, but the inclusion of this dissipation channel within the combined CLDM yields a very good agreement with experimental results. This is natural since in the real systems both dissipation channels are present. The combined CLDM gives also a better description of all the experimental data than the results of the lubrication theory with a correction factor for finite contact angles [31] which takes into account only the HD channel of dissipation, e.g., the root-mean-square deviation of the CLDM is 5.2 times smaller in Fig. 3 and 2.7 times smaller in Fig. 4 than that of the results in [31].

From the fitting of the experimental data by the combined CLDM we obtain here that the dissipation channel due to the moving contact line (the MKM) always dominates over the viscous flow dissipation (the HDM).

Recently in [30] it was obtained that near the critical velocity in the Wilhelmy-plate geometry the meniscus profile deviates from the quasistatic approximation. In the present approach one can take into account this by including in the differential equations the correction, related to the hydrodynamic change of the pressure of the free surface [3]. This will advance the CLDA outside the quasistatic approximation. However, this is beyond the scope of the present work and will be studied in a future work.

ACKNOWLEDGMENTS

S.I. has received financial support from the NSF-Bulgaria under Grant No. DO 02 75/08.

[1] C. Huh and L. E. Scriven, J. Colloid Interface Sci. **35**, 85 (1971).
[2] T. D. Blake and J. M. Haynes, J. Colloid Interface Sci. **30**, 421 (1969).
[3] O. V. Voinov, Fluid Dyn. **11**, 714 (1976).
[4] C. Huh and S. G. Mason, J. Fluid Mech. **81**, 401 (1977).
[5] L. M. Hocking, J. Fluid Mech. **79**, 209 (1977).
[6] H. P. Greenspan, J. Fluid Mech. **84**, 125 (1978).
[7] E. B. V. Dussan, Annu. Rev. Fluid Mech. **11**, 371 (1979).
[8] S. H. Davis, J. Appl. Mech., Trans. ASME **50**, 977 (1983).
[9] R. G. Cox, J. Fluid Mech. **168**, 169 (1986).
[10] Y. D. Shikhmurzaev, Phys. Fluids **9**, 266 (1997).
[11] I. B. Bazhlekov and P. J. Shopov, J. Fluid Mech. **352**, 113 (1997).
[12] P. G. de Gennes, Rev. Mod. Phys. **57**, 827 (1985).
[13] T. D. Blake, A. Clarke, J. De Coninck, and M. J. de Ruijter, Langmuir **13**, 2164 (1997).
[14] A. Milchev and K. Binder, J. Chem. Phys. **116**, 7691 (2002).
[15] P. Seppecher, Int. J. Eng. Sci. **34**, 977 (1996).
[16] A. Boudaoud, Eur. Phys. J. E **22**, 107 (2007).
[17] V. S. Nikolayev and D. A. Beysens, Phys. Rev. E **65**, 046135 (2002).
[18] N. Pesheva and J. De Coninck, Phys. Rev. E **70**, 046102 (2004).
[19] T. Blake, J. Colloid Interface Sci. **299**, 1 (2006).
[20] F. Brochard-Wyart and P. G. de Gennes, Adv. Colloid Interface Sci. **39**, 1 (1992).
[21] M. J. de Ruijter, J. De Coninck, and G. Oshanin, Langmuir **15**, 2209 (1999).
[22] J. F. Joanny and P.-G. de Gennes, J. Phys. (Paris) **47**, 121 (1986).
[23] M.-J. Vega, D. Seveno, G. Lemaur, M.-H. Ado, and J. De Coninck, Langmuir **21**, 9584 (2005).
[24] E. L. Decker and S. Garoff, Langmuir **13**, 6321 (1997).
[25] D. Quéré, Europhys. Lett. **39**, 533 (1997).
[26] P. G. Petrov and J. G. Petrov, Langmuir **11**, 3261 (1995).
[27] M. Schneemilch, R. A. Hayes, J. G. Petrov, and J. Ralston, Langmuir **14**, 7047 (1998).
[28] S. Moulinet, A. Rosso, W. Krauth, and E. Rolley, Phys. Rev. E **69**, 035103(R) (2004).
[29] S. Moulinet, C. Guthmann, and E. Rolley, Eur. Phys. J. B **37**, 127 (2003).
[30] M. Maleki, E. Reyssat, D. Quéré, and R. Golestanian, Langmuir **23**, 10116 (2007).
[31] G. Delon, M. Fermigier, J. Snoeijer, and B. Andreotti, J. Fluid Mech. **604**, 55 (2008).
[32] S. Iliev, N. Pesheva, and V. S. Nikolayev, Phys. Rev. E **78**, 021605 (2008).
[33] K. Sefiane, J. Skilling, and J. MacGillivray, Adv. Colloid Interface Sci. **138**, 101 (2008).
[34] B. W. Cherry and C. M. Holmes, J. Colloid Interface Sci. **29**, 174 (1969).
[35] P. G. de Gennes, Colloid Polym. Sci. **264**, 463 (1986).
[36] L. D. Landau and E. M. Lifshitz, *Fluid Mechanics* (Pergamon, Oxford, 1987).
[37] J. Snoeijer, B. Andreotti, G. Delon, and M. Fermigier, J. Fluid Mech. **579**, 63 (2007).
[38] S. Iliev, N. Pesheva, and V. S. Nikolayev, Phys. Rev. E **72**, 011606 (2005).
[39] H. Moffatt, J. Fluid Mech. **18**, 1 (1964).
[40] F. Domingues Dos Santos and T. Ondarçuhu, Phys. Rev. Lett. **75**, 2972 (1995).
[41] S. Iliev and N. Pesheva, Langmuir **22**, 1580 (2006).
[42] R. Golestanian and E. Raphaël, Phys. Rev. E **67**, 031603 (2003).
[43] R. Sedev and J. Petrov, Colloids Surf. **53**, 147 (1991).
[44] J. Snoeijer, Phys. Fluids **18**, 021701 (2006).
[45] D. Bonn, J. Eggers, J. Indekeu, J. Meunier, and E. Rolley, Rev. Mod. Phys. **81**, 739 (2009).